Determination of the CKM unitarity triangle by $B \to X_d l^+ l^-$ decay

L. T. Handoko*
Department of Physics, Hiroshima University, 1-3-1 Kagamiyama, Higashi Hiroshima - 739, Japan
(Received 20 June 1997; published 7 January 1998)

I examine the possibility to extract the angle γ of the Cabibbo-Kobayashi-Maskawa unitarity triangle by the inclusive $B \to X_d l^+ l^-$ decay. Independent information for the angle is expected from the nontrivial contribution induced in $u\bar{u}$ and $c\bar{c}$ loops. The contributions induce CP asymmetry which has a high sensitivity to the angle γ in the whole dilepton invariant mass region. Particularly, in the low dilepton invariant mass region, the sensitivity is also recognized in the branching ratio with any dilepton final states and the lepton polarization asymmetry with a dimuon final state. In the high dilepton invariant mass region, the sensitivity is tiny in all measurements with the exception of the CP asymmetry, which makes them good probes to confirm the measurement of $V_{td}^* V_{tb}$ in addition to the present data from B_d^0-$\bar{B}_d^0$ mixing. The decay rate and asymmetries are examined in the standard model taking into account the long-distance contributions due to vector mesons as well as its momentum dependences which would reduce the long-distance backgrounds in the channel. [S0556-2821(98)02403-5]

PACS number(s): 13.20.He, 12.15.Hh

I. INTRODUCTION

The hope that $B \to X_s l^+ l^-$ decay will be within experimental reach in the near future [1] encourages me to consider the $B \to X_d l^+ l^-$ decay. Both decays are important probes of the effective Hamiltonian governing the flavor-changing neutral current (FCNC) transition $b \to q l^+ l^-$ $(q = s, d)$ in the standard model (SM) as written below [2]:

$$\mathcal{H}_{\rm eff} = \frac{G_F \alpha}{\sqrt{2}\pi} V_{tq}^* V_{tb} \Bigg\{ C_9^{\rm eff} [\bar{q}\gamma_\mu L b][\bar{l}\gamma^\mu l] + C_{10}[\bar{q}\gamma_\mu L b] \times [\bar{l}\gamma^\mu \gamma_5 l] - 2C_7^{\rm eff} \left[\bar{q} i \sigma_{\mu\nu} \frac{\hat{q}^\nu}{\hat{s}} (R + \hat{m}_q L) b \right] \times [\bar{l}\gamma^\mu l] \Bigg\}, \tag{1}$$

where $L/R \equiv (1 \mp \gamma_5)/2$, q^μ denotes the four-momentum of the dilepton, $s = q^2$. A caret means normalization with m_b.

Theoretically, the most important interest in the $b \to d l^+ l^-$ decay is, that the matrix element contains unnegligible terms induced by the continuum part of $u\bar{u}$ and $c\bar{c}$ loops proportional to $V_{ud}^* V_{ub}$ and $V_{cd}^* V_{cb}$ [3]. These terms should give nontrivial contributions in the Wilson coefficient $C_9^{\rm eff}$ which induce CP violation in the channel. I call this contribution the CP violation factor (C_9^{CP}) throughout this paper. I will show that it can be utilized to determine the length x and the angle γ of the Cabibbo-Kobayashi-Maskawa (CKM) unitarity triangle in Fig. 1 at once. In this meaning, for example, the radiative $B \to X_d \gamma$ decay is not so useful since it gives only information for the length x that have already been measured well in B_d^0-$\bar{B}_d^0$ mixing. On the other hand, in the $b \to s l^+ l^-$ decay, C_9^{CP} is strongly suppressed due to the Glashow-Iliopoulos-Maiani (GIM) mechanism. Generally, rare B decays are clean processes to extract the CKM matrix elements, because nonperturbative effects in the decays are possibly tiny, less than a few percent as shown in [4] by using the heavy-quark effective theory approach.[1] In the analysis, I also utilize the experiment result of x_d in B_d^0-$\bar{B}_d^0$ mixing.

The purpose of this paper is to show a possibility to give an independent measurement for the angle γ of the CKM unitarity triangle in the SM by observing the channel. The calculation is done taking into account the q dependence in the long-distance (LD) contributions due to the vector mesons [5]. It is well known that including the q dependence, which has not been considered in the previous papers, will reduce the background due to LD contributions [6].

This paper is organized as follows. First I briefly describe the nontrivial contributions due to the resonance and continuum parts of $u\bar{u}$ and $c\bar{c}$ loops which induce C_9^{CP}. Next I consider the phenomenology of the contributions and its relation with the CKM unitarity triangle. Before summarizing, I analyze the decay rate and asymmetries, i.e., forward-backward (FB) asymmetry ($\bar{\mathcal{A}}_{\rm FB}$), CP asymmetry ($\bar{\mathcal{A}}_{CP}$) and lepton-polarization (LP) asymmetry ($\bar{\mathcal{A}}_{\rm LP}$) in the channel.

II. *CP* VIOLATION FACTOR

The effective Hamiltonian in Eq. (1) describes both inclusive $b \to q l^+ l^-$ decays by replacing q with s or d quarks respectively. In the SM, the QCD corrected Wilson coefficients which enter the physical decay amplitude above have

*On leave from P3FT-LIPI, Indonesia. Email address: handoko@theo.phys.sci.hiroshima-u.ac.jp

[1] I remind the reader that the approach is reliable only in the low dilepton mass region, but it is sufficient to justify the statement since in the high dilepton mass region the perturbative calculation is good.

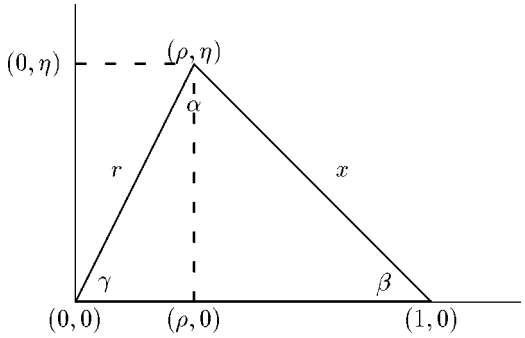

FIG. 1. The CKM unitarity triangle on the ρ-η plane.

been calculated up to next-to leading order (NLO) for $C_9{}^{\rm eff}$ and leading order (LO) for $C_7{}^{\rm eff}$ [7], while C_{10} does not receive any correction at all. Some corrections due to the continuum parts of $u\overline{u}$ and $c\overline{c}$ continuums and the resonances of the vector mesons will enter only in the coefficient $C_9{}^{\rm eff}$. Remember that the contribution of the $u\overline{u}$ loop in $C_7{}^{\rm eff}$ is suppressed because of the GIM mechanism [8].

Before giving $C_9{}^{\rm eff}$, related to the $u\overline{u}$ and $c\overline{c}$ loops, let me mention the operators which govern the $b\to q u^i \overline{u^i}$ processes,

$$\mathcal{O}_1=(\overline{q}_\alpha\gamma_\mu L b_\alpha)\sum_{i=1,2}(\overline{u^i_\beta}\gamma^\mu L u^i_\beta), \tag{2}$$

$$\mathcal{O}_2=(\overline{q}_\alpha\gamma_\mu L b_\beta)\sum_{i=1,2}(\overline{u^i_\beta}\gamma^\mu L u^i_\alpha), \tag{3}$$

after doing the Fierz transformation. Here, $u^1=u$, $u^2=c$, and the lower suffixes denote the color. For $q=s$, the $u\overline{u}$ loop contribution can be ignored [2,7], while for $q=d$ the situation is quite different. The reason is, that both operators above are proportional to the CKM matrix element $V^*_{u^i q}V_{u^i b}/V^*_{tq}V_{tb}$ if we normalize the amplitude with $V^*_{tq}V_{tb}$ as usual, then

$$\left|\frac{V^*_{u^i s}V_{u^i b}}{V^*_{ts}V_{tb}}\right|\sim\begin{cases}O(\lambda^2), & u^i=u,\\ O(1), & u^i=c,\end{cases} \tag{4}$$

for the former channel, and

$$\left|\frac{V^*_{u^i d}V_{u^i b}}{V^*_{td}V_{tb}}\right|\sim\begin{cases}O(1), & u^i=u,\\ O(1), & u^i=c,\end{cases} \tag{5}$$

for the latter one. λ is a parameter in the Wolfenstein parametrization of the CKM matrix [9] and the world average is $\lambda\sim 0.22$ [10].

Involving the continuum as well as the resonance parts of $u\overline{u}$ and $c\overline{c}$ loops and the NLO QCD correction into the calculation gives

$$C_9{}^{\rm eff}=C_9{}^{\rm NLO}\left[1+\frac{\alpha_s(\mu)}{\pi}\omega(\hat{s})\right]+C_9{}^{\rm con}(\hat{s})+C_9{}^{\rm res}(\hat{s}), \tag{6}$$

where

$$\begin{aligned}C_9{}^{\rm con}(\hat{s})=&\left[\left(1+\frac{V^*_{uq}V_{ub}}{V^*_{tq}V_{tb}}\right)g(\hat{m}_c,\hat{s})-\frac{V^*_{uq}V_{ub}}{V^*_{tq}V_{tb}}g(\hat{m}_u,\hat{s})\right]\\ &\times(3C_1+C_2+3C_3+C_4+3C_5+C_6)-\frac{1}{2}g(1,\hat{s})\\ &\times(4C_3+4C_4+3C_5+C_6)-\frac{1}{2}g(0,\hat{s})(C_3+3C_4)\\ &+\frac{2}{9}(3C_3+C_4+3C_5+C_6),\end{aligned} \tag{7}$$

$$\begin{aligned}C_9{}^{\rm res}(\hat{s})=&-\frac{16\pi^2}{9}(3C_1+C_2+3C_3+C_4\\ &+3C_5+C_6)\left[\left(1+\frac{V^*_{uq}V_{ub}}{V^*_{tq}V_{tb}}\right)\sum_{V=\psi,\ldots,}F_V(\hat{s})\right.\\ &\left.-\frac{V^*_{uq}V_{ub}}{V^*_{tq}V_{tb}}\sum_{V=\rho,\omega}F_V(\hat{s})\right].\end{aligned} \tag{8}$$

The readers should refer to [7] for $C_9{}^{\rm NLO}$ and

$$\begin{aligned}\omega(\hat{s})=&-\frac{2}{9}\pi^2-\frac{4}{3}{\rm Li}_2(\hat{s})-\frac{2}{3}\ln\hat{s}\ln(1-\hat{s})\\ &-\frac{5+4\hat{s}}{3(1+2\hat{s})}\ln(1-\hat{s})-\frac{2\hat{s}(1+\hat{s})(1-2\hat{s})}{3(1-\hat{s})^2(1+2\hat{s})}\ln\hat{s}\\ &+\frac{5+9\hat{s}-6\hat{s}^2}{6(1-\hat{s})(1+2\hat{s})}\end{aligned} \tag{9}$$

represents the $O(\alpha_s)$ correction from one gluon exchange in the matrix element of $\mathcal{O}_9$. The function $g(\hat{m}_{u^i},\hat{s})$ which describes the continuum part of the $u^i\overline{u^i}$ pair contribution is

$$\begin{aligned}g(\hat{m}_{u^i},\hat{s})=&-\frac{8}{9}\ln\left(\frac{m_b}{\mu}\right)-\frac{8}{9}\ln(\hat{m}_{u^i})+\frac{8}{27}+\frac{16}{9}\frac{\hat{m}^2_{u^i}}{\hat{s}}\\ &-\frac{2}{9}\left(2+\frac{4\hat{m}^2_{u^i}}{\hat{s}}\right)\sqrt{\left|1-\frac{4\hat{m}^2_{u^i}}{\hat{s}}\right|}\left[\Theta\left(1-\frac{4\hat{m}^2_{u^i}}{\hat{s}}\right)\right.\\ &\times\left(\ln\frac{1+\sqrt{1-4\hat{m}^2_{u^i}/\hat{s}}}{1-\sqrt{1-4\hat{m}^2_{u^i}/\hat{s}}}-i\pi\right)\\ &\left.+\Theta\left(\frac{4\hat{m}^2_{u^i}}{\hat{s}}-1\right)2\arctan\frac{1}{\sqrt{4\hat{m}^2_{u^i}/\hat{s}-1}}\right],\end{aligned} \tag{10}$$

$$g(0,\hat{s})=\frac{8}{27}-\frac{8}{9}\ln\left(\frac{m_b}{\mu}\right)-\frac{4}{9}\ln\hat{s}+\frac{4}{9}i\pi. \tag{11}$$

In the resonance part $C_9{}^{\rm res}$, I put the relative phase to be zero because of unitarity constraints in the Argand plot of the transition amplitude [5]. $F_V(\hat{s})$ is the Breit-Wigner resonance form

TABLE I. The experimental (central) values for each vector meson under consideration (upper) and the determined constants under these values (lower).

Parameter	Vector meson					
	ρ	ω	ψ	ψ'	ψ''	ψ'''
M_V (MeV)	768.5	781.94	3096.88	3686.00	3769.9	4040
$\Gamma_{e^+e^-}$ (keV)	6.77	0.6	5.26	2.14	0.26	0.75
Γ_V (MeV)	150.7	8.43	0.087	0.277	23.6	52
$P''_V(\hat{m}_V^2)$	-0.00243	-0.00243	-0.02734	-0.01463	-0.01374	-0.01153
$\hat{P}_V$	0.01339	0.01387	0.01577	0.01830	0.01885	0.02080
$\hat{f}_V(0)$	0.00662	0.00202	0.01795	0.01487	0.00536	0.01010

$$F_V(\hat{s})=\frac{\hat{f}_V^2(\hat{s})/\hat{s}}{\hat{s}-\hat{m}_V^2+i\hat{m}_V\hat{\Gamma}_V}. \tag{12}$$

$\hat{f}_V(\hat{s})$ describes the momentum dependence of the coupling strength of the vector interaction in the γ-V transition, i.e.,

$$\langle 0|\overline{u^i}\gamma_\mu u^i|V(q)\rangle\equiv f_V(q^2)\epsilon_\mu, \tag{13}$$

and has been derived as follows [6]:

$$\frac{\hat{f}_V(\hat{s})}{\hat{f}_V(0)}=1+\frac{\hat{s}}{\hat{P}_V}[P'_V-P''_V(\hat{s})], \tag{14}$$

under the assumption that the vector mesons are bound states of the pair $u^i\overline{u^i}$. Here,

$$P''_V(\hat{s})=\frac{\hat{m}_{u^i}^2}{4\pi^2\hat{s}}\left[-4-\frac{5\hat{s}}{3\hat{m}_{u^i}^2}+4\left(1+\frac{\hat{s}}{2\hat{m}_{u^i}^2}\right)\times\sqrt{\frac{4\hat{m}_{u^i}^2}{\hat{s}}-1}\arctan\frac{1}{\sqrt{4\hat{m}_{u^i}^2/\hat{s}-1}}\right] \tag{15}$$

is obtained from a dispersion relation involving the imaginary part of the quark-loop diagram, while P_V and P'_V are the subtraction constants. Kinematically the above interpolation equation of $\hat{f}_V$ is valid only for the $0\leqslant\hat{s}\leqslant\hat{m}_V^2$ region. For the $\hat{s}>\hat{m}_V^2$ region I use the same assumption found in [6]; that is, $\hat{f}_V(\hat{s}>\hat{m}_V^2)=\hat{f}_V(\hat{m}_V^2)$. In principle, the ratio in Eq. (14) should be obtained from the known data of the V production cross section by off-shell and on-shell photons.

The subtraction constants in Eq. (14) are written in the lower part of Table I for each vector meson. The results are determined by using the data in the upper table, putting $m_V\sim(2m_{u^i})$ and $P'_V=0.043$ for all V's. Unfortunately, there are no data of photoproduction for higher excited states of ψ, so let me use the same average value $|\hat{f}_V(0)/\hat{f}_V(\hat{m}_V^2)|\sim0.35$ for $V=\psi,\psi',\psi'',\psi'''$ and $|\hat{f}_V(0)/\hat{f}_V(\hat{m}_V^2)|\sim0.92$ for $V=\rho,\omega$ which fit the data on ρ,ω, and ψ [6]. This fact is also the reason why other resonances higher than ψ''' are not considered here. Otherwise, $\hat{f}_V(\hat{m}_V^2)$ can be obtained from the data on the leptonic width [10], that is,

$$\hat{f}_V^2(\hat{m}_V^2)=\frac{27\hat{m}_V^3}{16\pi\alpha^2}\hat{\Gamma}(V\rightarrow l^+l^-), \tag{16}$$

then $\hat{f}_V(0)$ would follow as written in Table I.

From Eqs. (7) and (8), it is obvious that $V_{uq}^*V_{ub}/V_{tq}^*V_{tb}$ would induce CP violation in the channel. For convenience, these terms can be collected as $(V_{uq}^*V_{ub}/V_{tq}^*V_{tb})C_9{}^{CP}(\hat{s})$, with

$$C_9{}^{CP}(\hat{s})=(3C_1+C_2+3C_3+C_4+3C_5+C_6)\times\left[g(\hat{m}_c,\hat{s})-g(\hat{m}_u,\hat{s})-\frac{16\pi^2}{9}\left(\sum_{V=\psi,\ldots,}F_V(\hat{s})-\sum_{V=\rho,\omega}F_V(\hat{s})\right)\right]. \tag{17}$$

Now let me derive some relations in the CKM unitarity triangle and give the numerical calculation for the auxiliary functions defined above. Especially it is worthwhile to see how large the contribution of $C_9{}^{CP}$ is. Using the Wolfenstein parametrization [9], one can rewrite the CKM factor as

$$\frac{V_{uq}^*V_{ub}}{V_{tq}^*V_{tb}}\sim\begin{cases}\dfrac{r(e^{-i\gamma}-r)}{1+r^2-2r\cos\gamma}, & q=d,\\ \lambda^2re^{-i\gamma}, & q=s.\end{cases} \tag{18}$$

As mentioned before, from Eqs. (4) and (18) it is obvious that in $b\rightarrow sl^+l^-$ decay, the $u\overline{u}$ loop and $C_9{}^{CP}$ is less important and negligible. In general one must treat r and γ as free parameters, while x must be determined by the data of B_d^0-$\overline{B_d^0}$ mixing. However, in the SM the unitarity triangle is satisfied in a good aproximation, so one can relate r and x to each other as

$$r=\sqrt{|x^2-\sin^2\gamma|}+\cos\gamma. \tag{19}$$

Here x is determined by the experimental value of x_d in B_d^0-$\overline{B_d^0}$ mixing, that is,

$$x=\left[\frac{x_d}{{G_F}^2/(6\pi^2)m_{B_d}{M_W}^2\tau_{B_d}\eta_{\rm QCD}{f_{B_d}}^2B_{B_d}|F_{\Delta B=2}|^2}\right]^{1/2}, \tag{20}$$

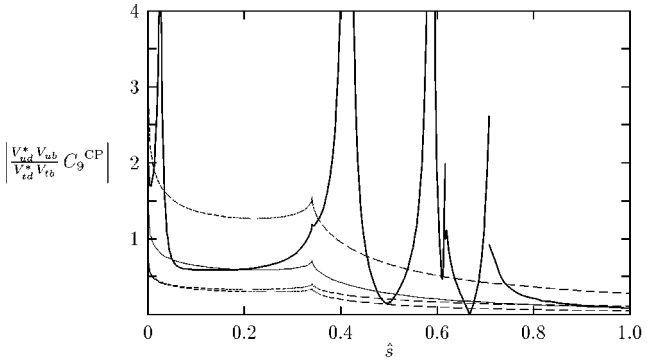

FIG. 2. The magnitude of $C_9{}^{CP}$ with (solid thick curve) and without (solid thin curve) resonances for $(\gamma,x)=(48.6°,0.778)$. The upper, middle and lower dashed curves show the magnitude without resonances for same x and $\gamma=0°,-90°,90°$.

with [11]

$$F_{\Delta B=2}=\frac{4-15x_t+12{x_t}^2-{x_t}^3-6{x_t}^2\ln x_t}{4(1-x_t)^3}, \qquad (21)$$

and $x_t=(m_t/m_W)^2$. For m_{B_d} and τ_{B_d}, I use m_{B^0} and τ_{B^0}.

The magnitude of $(V_{ud}^* V_{ub}/V_{td}^* V_{tb})C_9{}^{CP}$ as a function of $\hat{s}$ is depicted in Fig. 2. Here I use the following values for the Wilson coefficients:

$$C_1=-0.2404, \quad C_2=1.1032, \quad C_3=0.0107,$$

$$C_4=-0.0249, \quad C_5=0.0072,$$

$$C_6=-0.03024, \quad C_7{}^{\rm eff}=-0.3109, \quad C_8=-0.1478,$$

$$C_9{}^{\rm NLO}=4.1990, \quad C_{10}=-4.5399,$$

that are obtained by using the central values in Table II. The solid curves show the magnitude for $(\gamma,x)=(48.6°,0.778)$ which is the best fit in the SM up to now and equivalent to $(\rho,\eta)=(0.3,0.34)$. The upper, middle and lower dashed curves show the magnitude without LD effects with $\gamma=0°$, $-90°,90°$. It is obvious that the contribution is significant, about $\sim 20\%$ of $C_9{}^{\rm NLO}$ in the low $\hat{s}$ region ($\hat{s}<0.4$). Now, I am ready to analyze the decay rate and asymmetries in the channel.

III. DECAY RATE AND ASYMMETRIES

The double differential decay rate for semileptonic $B\to X_q l^+ l^-$ decay, involving the lepton and light quark masses, is expressed as

$$\frac{d^2\mathcal{B}(\hat{s},z)}{d\hat{s}dz}=\mathcal{B}_0\sqrt{1-\frac{4\hat{m}_l^2}{\hat{s}}}\hat{u}(\hat{s})\Bigg\{4[|C_9{}^{\rm eff}|^2-|C_{10}|^2]\hat{m}_l^2[1-\hat{s}+\hat{m}_q^2]+[|C_9{}^{\rm eff}|^2+|C_{10}|^2]\times\left[(1-\hat{m}_q^2)^2-\hat{s}^2-\hat{u}(\hat{s})^2\left(1-\frac{6\hat{m}_l^2}{\hat{s}}\right)z^2\right]$$
$$+4|C_7{}^{\rm eff}|^2\frac{1+2\hat{m}_l^2/\hat{s}}{\hat{s}}[1-\hat{m}_q^2-\hat{m}_q^4+\hat{m}_q^6-\hat{s}(8\hat{m}_q^2+\hat{s}+\hat{m}_q^2\hat{s})+\hat{u}(\hat{s})^2(1+\hat{m}_q^2)z^2]$$
$$-8{\rm Re}(C_9{}^{\rm eff})^* C_7{}^{\rm eff}\left[1+\frac{2\hat{m}_l^2}{\hat{s}}\right][\hat{s}(1+\hat{m}_q^2)-(1-\hat{m}_q^2)^2]+4C_{10}[{\rm Re}(C_9{}^{\rm eff})^*\hat{s}+2C_7{}^{\rm eff}(1+\hat{m}_q^2)]\hat{u}(\hat{s})z\Bigg\}, \qquad (22)$$

where $\hat{u}(\hat{s})=\sqrt{[\hat{s}-(1+\hat{m}_q)^2][\hat{s}-(1-\hat{m}_q)^2]}$, $z=\cos\theta$ is the angle of l^+ measured with respect to the b-quark direction in the dilepton c.m. system, and the normalization factor

$$\mathcal{B}_0=\mathcal{B}(B\to X_c l\bar{\nu})\frac{3}{16\pi^2}\frac{\alpha^2}{|V_{cb}|^2}\frac{|V_{tq}^* V_{tb}|^2}{f(\hat{m}_c)\kappa(\hat{m}_c)} \qquad (23)$$

is to reduce the uncertainty due to the b-quark mass. In the preceding notation, the CKM factor would read $|V_{td}^* V_{tb}|^2/|V_{cb}|^2\sim\lambda^2 x^2$. $f(\hat{m}_c)$ is the phase space function for $\Gamma(B\to X_c l\nu)$ in the parton model, while $\kappa(\hat{m}_c)$ accounts for the $O(\alpha_s)$ QCD correction to the decay. I write both functions explicitly as

$$f(\hat{m}_c)=1-8\hat{m}_c^2+8\hat{m}_c^6-\hat{m}_c^8-24\hat{m}_c^4\ln\hat{m}_c, \qquad (24)$$

$$\kappa(\hat{m}_c)=1-\frac{2\alpha_s(m_b)}{3\pi}\left[\frac{3}{2}+\left(\pi^2-\frac{31}{4}\right)(1-\hat{m}_c)^2\right], \qquad (25)$$

TABLE II. The values of parameters used throughout the paper.

Parameter	Value
m_W	80.26 ± 0.16 (GeV)
m_Z	91.19 ± 0.002 (GeV)
m_u	0.005 (GeV)
m_d	0.139 (GeV)
m_c	1.4 (GeV)
m_b	4.8 (GeV)
m_t	175 ± 9 (GeV)
m_e	0.511 (MeV)
m_μ	105.66 (MeV)
m_τ	$1777^{+0.30}_{-0.27}$ (MeV)
μ	$5^{+5.0}_{-2.5}$ (GeV)
$\Lambda^{(5)}_{\overline{QCD}}$	$0.214^{+0.066}_{-0.054}$ (GeV)
α^{-1}_{QED}	129
$\alpha_s(m_Z)$	0.117 ± 0.005
$\sin^2\theta_w$	0.2325
m_{B^0}	5279.2 ± 1.8 (MeV)
τ_{B^0}	1.28 ± 0.06 (ps)
$\eta_{\rm QCD}$	0.55
$\sqrt{f_{B_d}{}^2 B_{B_d}}$	173 ± 40 (MeV)
$\mathcal{B}(B\to X_c l\bar{\nu})$	$(10.4\pm0.4)\%$
x_d	0.73 ± 0.05

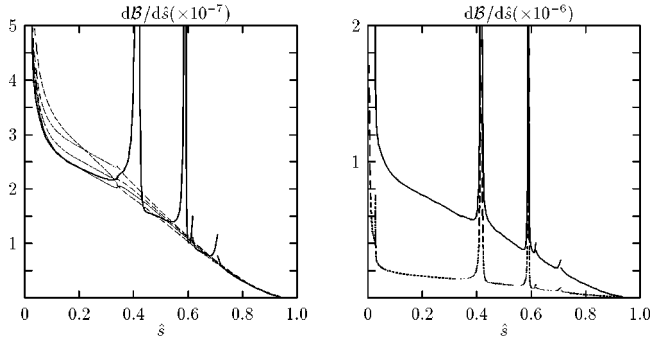

FIG. 3. Left: differential BR for e^+e^- with (thick curve) and without (thin curve) resonances for $(\gamma,x)=(48.6°,0.778)$. The upper, middle and lower dashed curves show the SD contribution for same x and $\gamma=0°,90°,-90°$. Right: same as the left for $\gamma=48.6°$ and $x=1.368$ (solid curve) and 0.631 (dashed curve).

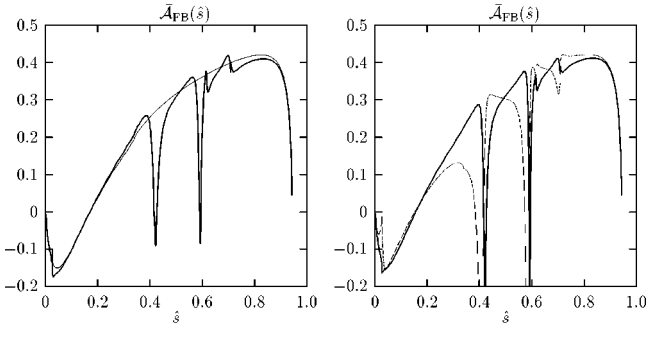

FIG. 4. Left: FB asymmetry for e^+e^- with (thick curve) and without (thin curve) resonances for $(\gamma,x)=(48.6°,0.778)$. Right: same with the left for same x and $\gamma=90°$ (solid line) and 0° (dashed line).

and use the values in Table II, $f(\hat{m}_c)=0.542$ and $\kappa(\hat{m}_c)=0.885$.

A. Decay rate

Now, let me consider the dilepton invariant mass distribution of the differential branching ratio (BR). It can be obtained by integrating Eq. (22) over the whole region of variable z,

$$\frac{d\mathcal{B}(\hat{s})}{d\hat{s}}=\int_{-1}^{1}dz\frac{d^2\mathcal{B}(\hat{s},z)}{d\hat{s}dz}. \tag{26}$$

This gives

$$\begin{aligned}\frac{d\mathcal{B}(\hat{s})}{d\hat{s}}=&\frac{4}{3}\mathcal{B}_0\sqrt{1-\frac{4\hat{m}_l^2}{\hat{s}}}\hat{u}(\hat{s})\Bigg\{6[|C_9{}^{\rm eff}|^2-|C_{10}|^2]\hat{m}_l^2[1-\hat{s}\\&+\hat{m}_q^2]+[|C_9{}^{\rm eff}|^2+|C_{10}|^2]\Bigg[(1-\hat{m}_q^2)^2+\hat{s}(1+\hat{m}_q^2)\\&-2\hat{s}^2+\hat{u}(\hat{s})^2\frac{2\hat{m}_l^2}{\hat{s}}\Bigg]+4|C_7{}^{\rm eff}|^2\frac{1+2\hat{m}_l^2/\hat{s}}{\hat{s}}\\&\times[2(1+\hat{m}_q^2)(1-\hat{m}_q^2)^2-(1+14\hat{m}_q^2+\hat{m}_q^4)\hat{s}\\&-(1+\hat{m}_q^2)\hat{s}^2]+12{\rm Re}(C_9{}^{\rm eff})^*C_7{}^{\rm eff}\Bigg[1+\frac{2\hat{m}_l^2}{\hat{s}}\Bigg]\\&\times[(1-\hat{m}_q^2)^2-(1+\hat{m}_q^2)\hat{s}]\Bigg\}.\end{aligned} \tag{27}$$

The distribution of differential BR's on the dilepton invariant mass for $B\to X_d e^+e^-$ is given in Fig. 3 for various values of γ and x. The high sensitivity on x is mostly coming from the CKM factor in Eq. (23), while the sensitivity on γ seems significant only in the low $\hat{s}$ region. Then, in the high $\hat{s}$ region the differential BR may be a good test for x and makes the loss of B_d^0-$\overline{B_d^0}$ mixing because of the theoretical uncertainties in the treatment of hadron matrix element $\langle B|\mathcal{O}^\dagger\mathcal{O}|B\rangle$ good. I have made certain that the momentum dependence of resonances in the channel is not as large as the result in [6]. There is only a $\sim 4\%$ reductioon compared with using $\hat{f}_V(\hat{m}_V^2)$ for all of the region. This is because of the $1/\hat{s}$ suppression in Eq. (12) [12].

Next, I am going to examine some measurements that are sensitive to γ and less sensitive to x. This may be achieved by considering the asymmetries and normalizing them with the differential BR to eliminate the CKM factor.

B. Forward-backward asymmetry

First, I provide the FB asymmetry. The normalized FB asymmetry is defined as follows [13]:

$$\begin{aligned}\overline{\mathcal{A}_{\rm FB}}(\hat{s})=&\frac{\int_0^1 dz[d^2\mathcal{B}(\hat{s},z)/d\hat{s}dz]-\int_{-1}^0 dz[d^2\mathcal{B}(\hat{s},z)/d\hat{s}dz]}{\int_0^1 dz[d^2\mathcal{B}(\hat{s},z)/d\hat{s}dz]+\int_{-1}^0 dz[d^2\mathcal{B}(\hat{s},z)/d\hat{s}dz]}\\=&\frac{d\mathcal{A}_{\rm FB}(\hat{s})/d\hat{s}}{d\mathcal{B}(\hat{s})/d\hat{s}}.\end{aligned} \tag{28}$$

Then, after integrating Eq. (27) properly, the nominator reads

$$\begin{aligned}\frac{d\mathcal{A}_{\rm FB}(\hat{s})}{d\hat{s}}=&-4\mathcal{B}_0\sqrt{1-\frac{4\hat{m}_l^2}{\hat{s}}}\hat{u}(\hat{s})^2C_{10}[{\rm Re}(C_9{}^{\rm eff})^*\hat{s}\\&+2C_7{}^{\rm eff}(1+\hat{m}_q^2)].\end{aligned} \tag{29}$$

In Fig. 4, I plot the FB asymmetry for $B\to X_d e^+e^-$ with and without the resonances on the left, while on the right with varying γ and keeping x constant.

C. *CP* asymmetry

Using the same treatment as in [3] in the amplitude level, the normalized CP asymmetry can be written simply as

$$\begin{aligned}\overline{\mathcal{A}_{CP}}(\hat{s})=&\frac{d\mathcal{B}(\hat{s})/d\hat{s}-d\overline{\mathcal{B}}(\hat{s})/d\hat{s}}{d\mathcal{B}(\hat{s})/d\hat{s}+d\overline{\mathcal{B}}(\hat{s})/d\hat{s}}\\=&\frac{-2d\mathcal{A}_{CP}(\hat{s})/d\hat{s}}{d\mathcal{B}(\hat{s})/d\hat{s}+2d\mathcal{A}_{CP}(\hat{s})/d\hat{s}},\end{aligned} \tag{30}$$

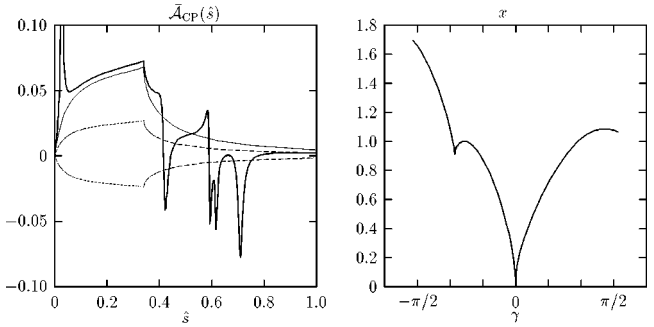

FIG. 5. Left: CP asymmetry for e^+e^- with (solid thick curve) and without (solid thin curve) resonances for $(\gamma,x)=(48.6°,0.778)$. The upper and lower dashed curves show the SD contribution for same x and $\gamma=90°,-90°$. Right: x as a function of γ where $\overline{\mathcal{A}_{CP}}=0$. The dashed lines denote the upper and lower bounds of x in the SM.

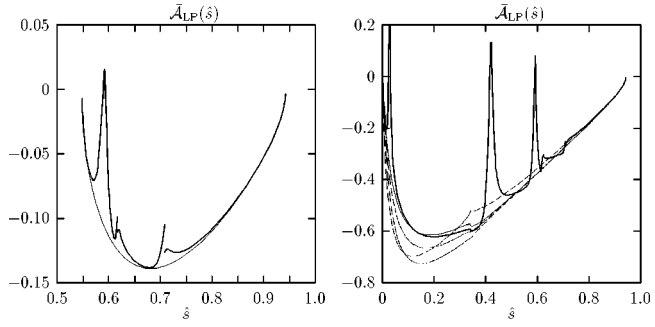

FIG. 6. Left: LP asymmetry for $\tau^+\tau^-$ with (solid thick curve) and without (solid thin curve) resonances for $(\gamma,x)=(48.6°,0.778)$. Right: same as the left but for $\mu^+\mu^-$. The dashed curves show the SD contribution for the same x and $\gamma=0°,90°,-90°$.

where $\mathcal{B}$ and $\overline{\mathcal{B}}$ denote the BR of $\overline{b}\to q l^+ l^-$ and its complex conjugate $b\to\overline{q}\, l^+ l^-$, respectively. For convenience, $C_9{}^{\rm eff}$ is divided into two terms according to the factor $V_{uq}^* V_{ub}/V_{tq}^* V_{tb}$:

$$C_9{}^{\rm eff}=\overline{C_9}+\frac{V_{uq}^* V_{ub}}{V_{tq}^* V_{tb}} C_9{}^{CP}. \tag{31}$$

Then, the result for the differential CP asymmetry is

$$\begin{aligned}\frac{d\mathcal{A}_{CP}(\hat{s})}{d\hat{s}}=&\frac{4}{3}\mathcal{B}_0\sqrt{1-\frac{4\hat{m}_l^2}{\hat{s}}}\hat{u}(\hat{s})\,{\rm Im}\left[\frac{V_{uq}^* V_{ub}}{V_{tq}^* V_{tb}}\right]\\ &\times\Bigg\{{\rm Im}[\overline{C_9}^* C_9{}^{CP}]\Bigg[(1-\hat{m}_q^2)^2+\hat{s}(1+\hat{m}_q^2)\\ &-2\hat{s}^2+\hat{u}(\hat{s})^2\frac{2\hat{m}_l^2}{\hat{s}}+6\hat{m}_l^2(1-\hat{s}+\hat{m}_q^2)\Bigg]\\ &+6\,{\rm Im}[C_7{}^{\rm eff} C_9{}^{CP}]\Bigg[1+\frac{2\hat{m}_l^2}{\hat{s}}\Bigg][(1-\hat{m}_q^2)^2\\ &-(1+\hat{m}_q^2)\hat{s}]\Bigg\}.\end{aligned} \tag{32}$$

In Fig. 5, I give the distribution of $\overline{\mathcal{A}_{CP}}$ (left figure) with (solid thick line) and without (solid thin line) resonances. It is easily understood that in the present case the dependence on γ is large, because of the appearance of the factor $r\sin\gamma$ from the CKM factor in Eq. (32). Moreover, it is clear that $\overline{\mathcal{A}_{CP}}$ will be nonzero if the imaginary part of Eq. (18) is nonzero. Anyway, a condition that $\overline{\mathcal{A}_{CP}}=0$ for $q=d$ in the SM is satisfied by the following equation:

$$x^2=\sin^2\gamma\left[1+\frac{1}{4}(1-\sqrt{|3+4\cot\gamma|})^2\right], \tag{33}$$

by using Eq. (19). The right part of Fig. 5 is plotted based on this equation. As depicted in the figure, there are still allowed regions of γ where $\overline{\mathcal{A}_{CP}}=0$. Notice again that from Eq. (18), $\overline{\mathcal{A}_{CP}}(B\to X_s l^+ l^-)$ would be $\sim 5\%$ of $\overline{\mathcal{A}_{CP}}(B\to X_d l^+ l^-)$ because of the suppression of λ^2.

D. Lepton-polarization asymmetry

Up to now, all of the measurements have been less sensitive to the lepton mass. Next, I provide the LP asymmetry which must be considered for the heavy dilepton final state and is proposed first in [14] for $B\to X_s\tau^+\tau^-$. Generally, the normalized LP asymmetry is given as

$$\overline{\mathcal{A}_{\rm LP}}(\hat{s})=\frac{d\mathcal{B}(\hat{s},\boldsymbol{n})/d\hat{s}-d\mathcal{B}(\hat{s},-\boldsymbol{n})/d\hat{s}}{d\mathcal{B}(\hat{s},\boldsymbol{n})/d\hat{s}+d\mathcal{B}(\hat{s},-\boldsymbol{n})/d\hat{s}}=\frac{d\mathcal{A}_{\rm LP}(\hat{s})/d\hat{s}}{d\mathcal{B}(\hat{s})/d\hat{s}}, \tag{34}$$

with $\boldsymbol{n}$ is a unit vector of any given spin direction of l^- in its rest frame. Then, for the longitudinal polarization, where $\boldsymbol{n}$ has the same direction with the momentum of l^- ($\boldsymbol{p}_{l^-}$),

$$\begin{aligned}\frac{d\mathcal{A}_{\rm LP}(\hat{s})}{d\hat{s}}=&\frac{8}{3}\mathcal{B}_0\left(1-\frac{4\hat{m}_l^2}{\hat{s}}\right)\hat{u}(\hat{s})C_{10}\{6C_7{}^{\rm eff}[(1-\hat{m}_q^2)^2\\ &-\hat{s}(1+\hat{m}_q^2)]+{\rm Re}(C_9{}^{\rm eff})^*[(1-\hat{m}_q^2)^2\\ &+\hat{s}(1+mq^2)-2\hat{s}^2]\}.\end{aligned} \tag{35}$$

The distribution is depicted in Fig. 6. As shown in the figure, for the $\tau^+\tau^-$ final state the sensitivity on γ is tiny. The reason is that for the $\tau^+\tau^-$ final state the distribution starts appearing in a region higher than $\hat{s}=(4\hat{m}_\tau{}^2)$. On the other hand, generally the high sensitivity on γ is expected in the low $\hat{s}$ region. So it may be interesting to consider the transversal polarization which has a different structure [14]. Unfortunately, I have checked, and the transversal lepton polarization asymmetry is too small for a light dilepton such as $\mu^+\mu^-$, so one must consider $\tau^+\tau^-$ again, the distribution which is limited for higher $\hat{s}$ regions.

IV. SUMMARY

I have shown how to extract the angle γ of the CKM unitarity triangle by inclusive $B\to X_d l^+ l^-$ decay and the data

of x_d in the SM. As a result, I can finally make the following points.

(1) For the low $\hat{s}$ region, i.e., $0.1<\hat{s}<0.3$, 5–10 % discrepancies in $\mathcal{B}(B\to X_d e^+ e^-)$ and $\overline{\mathcal{A}_{\rm LP}}(B\to X_d \mu^+ \mu^-)$ may be good signals for the CP violation factor defined here.

(2) According to the fact that the sensitivity on γ in the high $\hat{s}$ region, i.e., $\hat{s}>0.6$, is tiny, a measurement of x may be done by exploring one of the measurements discussed in the present paper in addition to the present data of x_d in $B_d^0 - \overline{B_d^0}$ mixing.

(3) CP violation asymmetry in the channel should measure the dependence on γ. It will, at least, be a good probe to determine the sign of the angle γ.

To conclude, the measurements of the decay rate and asymmetries in $B\to X_d l^+ l^-$ decay will provide independent information for γ. This information is a crucial test of CKM unitarity as well as leading to the discovery of unitarity violation.

ACKNOWLEDGMENTS

I thank T. Muta for reading the manuscript, M. R. Ahmady and Y. Kiyo for useful discussion on q dependence in the long distance effects and D. X. Zhang for pointing out the $1/q^2$ dependence in the leptonic decay of vector mesons. I also would like to thank the Particle Elementary Physics Group for the warm hospitality during my stay at ICTP Italy during the last stages of this work and the Ministry of Education, Science and Culture (Monbusho-Japan) for financial support.

[1] A. Ali, talk given at the *4th KEK Topical Conference on Flavor Physics*, Tsukuba, Japan (unpublished), and references therein.

[2] B. Grinstein, M. J. Savage, and M. B. Wise, Nucl. Phys. **B319**, 271 (1989); R. Grigjanis, P. J. O'Donnel, M. Sutherland, and H. Navelt, Phys. Lett. B **223**, 239 (1989).

[3] F. Krüger and L. M. Sehgal, Phys. Rev. D **55**, 2799 (1997).

[4] A. V. Manohar and M. B. Wise, Phys. Rev. D **49**, 1310 (1994); A. Ali, G. Hiller, L. T. Handoko, and T. Morozumi, *ibid.* **55**, 4105 (1997).

[5] C. S. Lim, T. Morozumi, and A. I. Sanda, Phys. Lett. B **218**, 343 (1989); N. G. Deshpande, J. Trampetic, and K. Panose, Phys. Rev. D **39**, 1461 (1989); P. J. O'Donnell and H. K. K. Tung, *ibid.* **43**, R2067 (1991); P. J. O'Donnell, M. Sutherland, and K. K. Tung, *ibid.* **46**, 4091 (1992).

[6] K. Terasaki, Nuovo Cimento A **66**, 475 (1981): N. G. Deshpande, X. G. He, and J. Trampetic, Phys. Lett. B **367**, 362 (1996); M. R. Ahmady, Phys. Rev. D **53**, 2843 (1996).

[7] M. Jżabek and J. H. Kühn, Nucl. Phys. **B320**, 20 (1989); M. Misiak, *ibid.* **B393**, 23 (1993); **B439**, 461(E) (1995); A. J. Buras and M. Münz, Phys. Rev. D **52**, 186 (1995).

[8] T. Inami and C. S. Lim, Philos. Trans. R. Soc. London, Ser. A **65**, 297 (1981).

[9] L. Wolfenstein, Phys. Rev. Lett. **51**, 1945 (1983).

[10] Particle Data Group, R. M. Barnett *et al.* Phys. Rev. D **54**, 1 (1996).

[11] B. A. Campbell and P. J. O'Donnell, Phys. Rev. D **25**, 1989 (1982); A. J. Buras and M. K. Harlander, in *Heavy Flavours*, edited by A. J. Buras and M. Lindner (World Scientific, Singapore, 1992), p. 58,

[12] C. D. Lü and D. X. Zhang, Phys. Lett. B **397**, 279 (1997).

[13] A. Ali, T. Mannel and T. Morozumi, Phys. Lett. B **373**, 505 (1991).

[14] J. L. Hewett, Phys. Rev. D **53**, 4964 (1996): F. Krüger and L. M. Sehgal, Phys. Lett. B **380**, 199 (1996).